

To be published in Optics Express:

Title: Single and multi-pulse based X-ray Photon Correlation Spectroscopy

Authors: Wonhyuk Jo, Stephan Stern, FABIAN WESTERMEIER, Rustam Rysov, Matthias Riepp, Julian Schmeh, Jörn Lange, Julian Becker, Michael Sprung, Torsten Laurus, Heinz Graafsma, Irina Lokteva, Gerhard Gruebel, Wojciech Roseker

Accepted: 13 December 22

Posted 14 December 22

DOI: <https://doi.org/10.1364/OE.477774>

© 2022 Optica Publishing Group under the terms of the [Optica Open Access Publishing Agreement](#)

OPTICA
PUBLISHING GROUP
Formerly OSA

Single and multi-pulse based X-ray Photon Correlation Spectroscopy

WONHYUK JO,^{1,4,6} STEPHAN STERN,² FABIAN WESTERMEIER,¹
RUSTAM RYSOV,¹ MATTHIAS RIEPP,^{1,5} JULIAN SCHMEHR,² JÖRN
LANGE,² JULIAN BECKER,² MICHAEL SPRUNG,¹ TORSTEN LAURUS,¹
HEINZ GRAAFSMA,¹ IRINA LOKTEVA,^{1,3} GERHARD GRÜBEL,^{1,3,4} AND
WOJCIECH ROSEKER^{1,7}

¹Deutsches Elektronen-Synchrotron DESY, Notkestraße 85, 22607 Hamburg, Germany

²X-Spectrum GmbH, Luruper Hauptstraße 1, 22547 Hamburg, Germany

³The Hamburg Centre for Ultrafast Imaging, Luruper Chaussee 149, 22761 Hamburg, Germany

⁴Current affiliation: European X-ray Free Electron Laser GmbH, Holzkoppel 4, 22869, Schenefeld, Germany

⁵Current affiliation: Université de Strasbourg, CNRS, Institut de Physique et Chimie des Matériaux de Strasbourg, UMR 7504, F-67000 Strasbourg, France

⁶wonhyuk.jo@xfel.eu

⁷wojciech.roseker@desy.de

Abstract: The ability of pulsed nature of synchrotron radiation opens up the possibility of studying microsecond dynamics in complex materials via speckle-based techniques. Here, we present the study of measuring the dynamics of a colloidal system by combining single and multiple X-ray pulses of a storage ring. In addition, we apply speckle correlation techniques at various pulse patterns to collect correlation functions from nanoseconds to milliseconds. The obtained sample dynamics from all correlation techniques at different pulse patterns are in very good agreement with the expected dynamics of Brownian motions of silica nanoparticles in water. Our study will pave the way for future pulsed X-ray investigations at various synchrotron X-ray sources using individual X-ray pulse patterns.

© 2022 Optica Publishing Group under the terms of the [Optica Open Access Publishing Agreement](#)

1. Introduction

Speckle-based techniques are well established to investigate sample dynamics in soft matter. The high coherence beam leaves an imprint of the spatial distribution of the subjected system on a diffraction image as a grainy interference pattern at the detector plane, which is typically called “speckle”. The movement of disordered particles shifts the relative phases of the scattered field and induces temporal variations in the speckle patterns. Consequently, these fluctuating speckle intensities reflect the information of the system dynamics, which can be quantified by a correlation function. For many decades, optical laser systems have been widely employed to generate speckle patterns for photon correlation spectroscopy (PCS) [1–3]. Thanks to the improvement of the coherent X-ray flux from synchrotron sources, X-rays have been employed for speckle-based measurements of dynamics on the atomic scale [4] or optically turbid system [5].

One of the most robust techniques, called X-ray photon correlation spectroscopy (XPCS), is a powerful and convenient tool for measuring dynamics. The temporal resolution of the technique is defined by the number of images taken in time. In the past decades, considerably slow systems have been in the focus of XPCS studies [6–14]. Recently, new advanced detector technology has begun to offer 2D detectors with the microsecond temporal resolutions in XPCS measurements (e.g., VIPIC [15], UFXC32k [16], Tristan detector [17], and the XSPA-500k [18]). Recently developed X-ray detectors offering MHz frame rates, such as adaptive gain integrated pixel detector (AGIPD), enable to investigate of nanosecond colloidal dynamics at 3rd generation X-ray

synchrotron sources [19] and X-ray free electron laser (XFEL) sources [20,21]. In order to measure sample dynamics faster than accessible with XPCS, X-ray speckle visibility spectroscopy (XSVS) has been developed, which evaluates a speckle contrast as a function of illumination time. The longer illumination time compared to system dynamics leads the more blurred speckle images and a loss in contrast of the speckle images. This concept was introduced in optical laser systems [22] and extended to X-ray regime [23–27].

An alternative speckle technique is double pulse XPCS (DP-XPCS). The technique evaluates a speckle contrast of two summed speckle patterns separated with a delay time, which corresponds to the temporal resolution. DP-XPCS has been demonstrated with sequentially obtained speckle patterns [28] and an optical pulse laser scheme [29]. More recently, DP-XPCS has been employed in a special operation mode of linear accelerators of XFEL [30, 31] or X-ray split-and-delay unit [32–42] to investigate nanosecond dynamics beyond detector frame rate limitations.

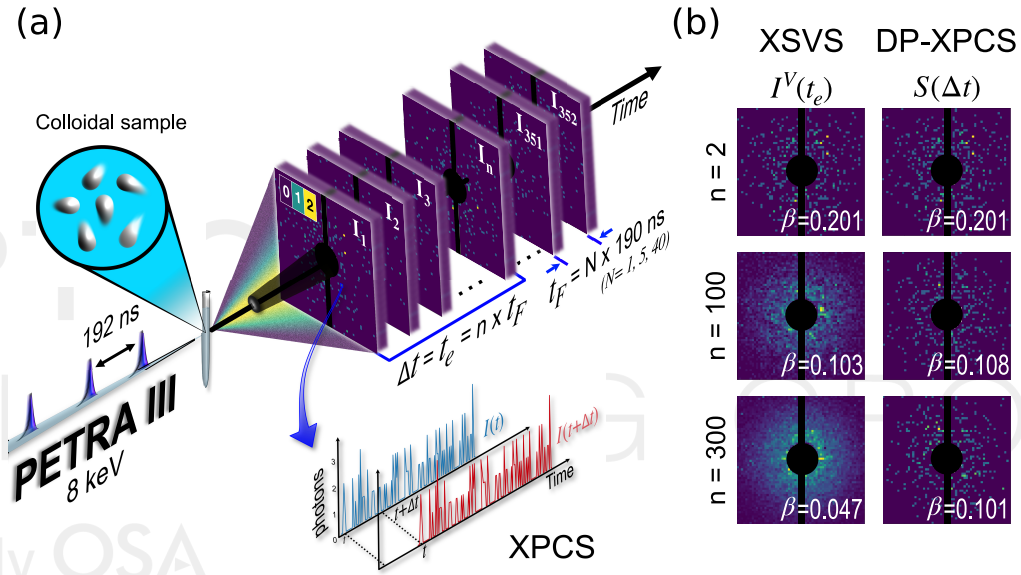


Fig. 1. (a) Schematics of the speckle measurement experiment employing the intrinsic pulse structure of PETRA III. Coherent X-ray pulses are delivered at the sample position with 192 ns temporal separation. SPARTA collects 352 images in a single measurement, and the delay time between each frame is set by the number of X-ray pulses between two consecutive frames N . (b) Speckle images of XSVS and DP-XPCS for N_{40} with varying number of frames n .

N	Δt
1 (N_1 , Single pulse mode)	192 ns - 67.6 μ s
5 (N_5 , 5 pulse mode)	960 ns - 338 μ s
40 (N_{40} , Revolution mode)	7.68 μ s - 2.7 ms

Table 1. Data collection modes of SPARTA. N and Δt denote the number of X-ray pulses between two successive frames and the time range of correlation functions, respectively.

In this paper, we demonstrated XPCS measurements using single and multiple X-ray pulses

from nanoseconds to milliseconds time scales. Thanks to the MHz frame rate of the detector, we investigated the sample dynamics with 192 ns temporal resolution in a single pulse mode. In addition, we covered the gap between nanoseconds to milliseconds using the multiple X-ray pulse modes in the correlation function. The obtained sample dynamics are in excellent agreement with the expected dynamics of the system.

2. Materials and Methods

2.1. Experiments

The experiment was conducted at the coherent application beamline P10 of PETRA III [43]. The monochromatic 8 keV X-ray beam was focused vertically and horizontally down to $d_b = 2.5 \mu\text{m}$ at the sample position. The speckle size $d_s = 310 \mu\text{m}$ was estimated at the detector plane located at a distance $L = 5 \text{ m}$, according to $d_s = \lambda L / d_b$, where λ is the X-ray wavelength. The silica colloidal nanoparticles (NPs) with a core radius R of 65 nm were dispersed in water and filled in a $700 \mu\text{m}$ thick quartz capillary. The SPARTA detector, which was developed by the X-Spectrum GmbH with AGIPD technology [44–46] was employed to measure the sample dynamics. The detector is composed of 128×512 pixels with a pixel size of $200 \mu\text{m} \times 200 \mu\text{m}$. It can collect up to 352 memory cells (i.e., frames) at a frame rate in the MHz range in a single burst (i.e., measurement). The images have to be read out until the next MHz acquisition burst can be triggered 0.1 s later. Note that the number of X-ray pulses (N) between two consecutive frames adjusts the time resolution and the achievable time window in correlation functions. In this work, we selected $N = 1, 5$, and 40 to capture the sample dynamics (see supplement Fig. S1 and Tab. 1). The detector signal was carefully extracted using a background subtraction method that is elaborated elsewhere [19, 21] and subsequent conversion of the cleaned signal to an integer number of photons. An additional pixel mask was applied in the analysis to exclude detector pixels with high electronic noise. The depicted speckle patterns after the data conversion process to photons are shown in Fig. 1(b).

2.2. X-ray photon correlation spectroscopy

Three complementary XPCS techniques (i.e., XPCS, XSVS, and DP-XPCS) were employed to evaluate the sample dynamics obtained from different collection modes.

2.2.1. XPCS

The intensity fluctuations in time are caused by the spatial rearrangement of colloidal particles. The sample dynamic properties are traced by the intensity autocorrelation function together with the Siegert relation [47, 48]

$$g^{(2)}(Q, \Delta t) = \frac{\langle I(Q, t) I(Q, t + \Delta t) \rangle}{\langle I(Q, t) \rangle^2} = 1 + \beta_0 |f(Q, \Delta t)|^2, \quad (1)$$

where $I(Q, t)$ denotes the intensity of the speckle pattern at wavevector Q and time t . The bracket $\langle \rangle$ stands for time averaging, and Δt represents a delay time. The wavevector Q is defined by λ and scattering angle 2θ according to $Q = 4\pi \sin(\theta) / \lambda$. The β_0 is the speckle contrast mostly defined by the degree of coherence of the beam and experimental configuration [49, 50]. For the simple monodisperse colloidal case, the intermediate scattering function (ISF: $f(Q, \Delta t)$) is considered via a simple exponential decay function

$$f(Q, \Delta t) = \exp(-\Gamma(Q)\Delta t), \quad (2)$$

where $\Gamma(Q) = D_0 Q^2$ for typical Brownian motion and D_0 is defined by the Stokes-Einstein relation as $D_0 = \frac{k_b T}{6\pi\eta R}$, where k_b , T , η are the Boltzmann constant, environment temperature and medium viscosity, respectively. Note that in the limit of $\Delta t \rightarrow 0$, the $g^{(2)} - 1$ corresponds to the $\beta_0(\Delta t = 0)$ and decreases as a function of Δt taking into account the sample dynamics that can be expressed as

$$\beta_0 \exp(-2\Gamma\Delta t) = g^{(2)}(Q, \Delta t) - 1. \quad (3)$$

The obtained correlation function provides the contrast $\beta^C(Q, \Delta t) = \beta_0 \exp(-2\Gamma(Q)\Delta t)$ that starts with β_0 and decreases as a function of Δt due to the sample dynamics.

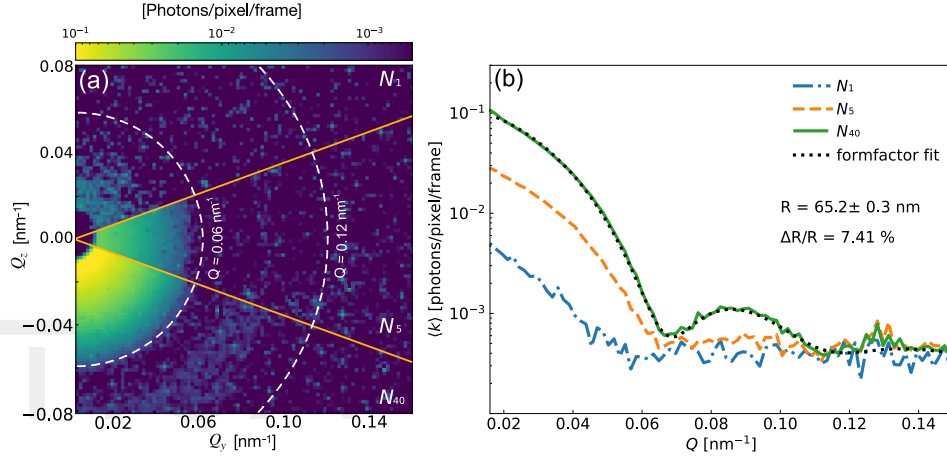


Fig. 2. (a) 2D speckle pattern taken by SPARTA for N_1 , N_5 , and N_{40} . (b) Corresponding azimuthally integrated intensity profiles as a function of Q . The black dotted line represents the formfactor fit, taking into account the sample polydispersity ($\Delta R/R$).

2.2.2. X-ray speckle visibility spectroscopy

In order to investigate system dynamics using XSVS from sequentially obtained speckle patterns, a speckle image with an exposure time t_e is defined as $I^V(Q, t_e) = \int_t^{t+t_e} I(Q, t') dt' = \sum_n^{n+n_e} I(Q, n)$, where $t_e = 190 \text{ ns} \times n_e N$, and n_e is the number of frames corresponding to t_e . The extending of t_e does not affect the speckle contrast until the sample characteristic time Γ^{-1} is sufficiently smaller than t_e . In contrast, when $t_e > \Gamma^{-1}$, the speckle image is washed out, and consequently, the contrast decreases. In Fig. 1 (b), the degrading of speckle image clarity as a function of n is clearly observed, and the normalized variance $\beta \equiv M^{-1} = \sigma^2(I^V)/\langle I^V \rangle^2$, where M is a number of speckle mode in the intensity is given by [22, 51, 52]

$$\beta_V(Q, \Delta t) = \frac{2\beta_0}{t_e} \int_0^{t_e} (1 - t/t_e) |f(Q, \Delta t)|^2 dt. \quad (4)$$

In case of the simple exponential decay function $f(Q, \Delta t) = \exp(-\Gamma\Delta t)$, Eq. 4 can be solved analytically as

$$\beta_V(Q, \Delta t) = \frac{\beta_0}{2\Gamma^2 t_e^2} [2\Gamma t_e - 1 + \exp(-2\Gamma t_e)]. \quad (5)$$

Note that the Eq. 5 shows more moderate decay in contrast compared to the β^C .

2.2.3. Double pulse XPCS

Double pulse speckle contrast β from the sum of two speckle patterns $S(Q, \Delta t) = I(Q, t) + I(Q, t + \Delta t)$ enables to quantify the level of displacements of colloidal particles within the delay time Δt . The contrast is given by the normalized variance of intensity distribution at a wavevector Q evaluated as [28]

$$c_2(Q, \Delta t) = \frac{\langle S^2(Q, \Delta t) \rangle - \langle S(Q, \Delta t) \rangle^2}{\langle S(Q, \Delta t) \rangle^2} = \frac{\beta_0}{2}(1 + |f(Q, \Delta t)|^2) + \alpha, \quad (6)$$

where α is the shot noise.

For weak speckle patterns, the photon counting statistics should be accounted for. The probability distribution of the number of photons per pixel k in a speckle pattern is described by the negative binomial distribution function [53]

$$P_{NB}(k) = \frac{\Gamma(k + M)}{\Gamma(M)\Gamma(k + 1)} \left(1 + \frac{M}{\langle k \rangle}\right)^{-k} \left(1 + \frac{\langle k \rangle}{M}\right)^{-M}. \quad (7)$$

In the negative binomial distribution, the normalized variance can be expressed as $M^{-1} = \sigma^2(k)/\langle k \rangle^2 - 1/\langle k \rangle$ [4].

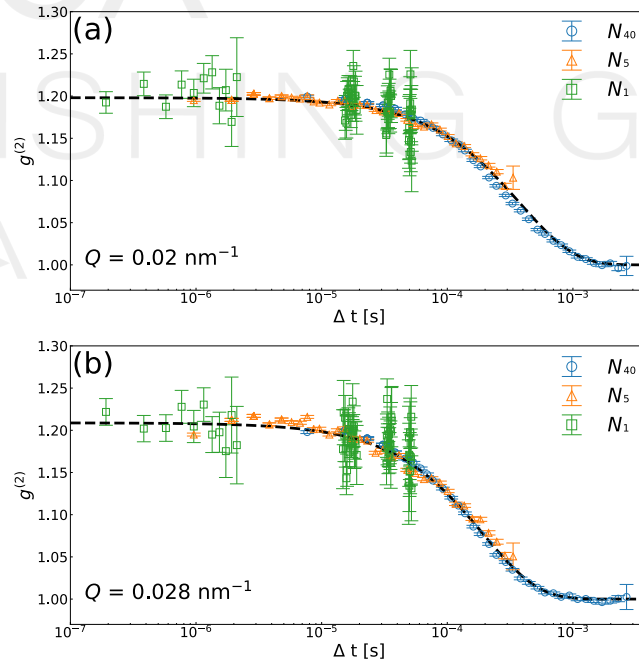


Fig. 3. Intensity correlation functions as a function of delay time obtained from N_1 (green-square), N_5 (orange-triangle), and N_{40} (blue-circle) for $Q = 0.02 \text{ nm}^{-1}$ (a) and 0.028 nm^{-1} (b). The dashed lines indicate the expected correlation functions using Eq. 3.

3. Result and discussion

Figure 2 (a) shows the averaged intensity collected at the N_1 , N_5 , and N_{40} , respectively. A total of 4700 bursts were employed to obtain a sufficient signal-to-noise ratio for N_1 and N_5 , and 470 bursts were used for N_{40} . The azimuthally integrated intensity profiles are shown in Fig. 2 (b). The intensity profiles fall off as a function of Q . The particle formfactor ring is well pronounced at $Q = 0.09 \text{ nm}^{-1}$ for N_{40} , indicating a system of sufficiently dilute and non-interacting silica particles. A single-sphere formfactor fit to the intensity profile obtained with N_{40} yields $R = 65.2 \pm 0.3 \text{ nm}$ and size polydispersity $\Delta R/R = 7.41 \%$.

We divided the detector plane into regions of interest (ROI) that are limited by contours of equivalent wavevector Q for further analysis.

Figure 3 shows $g^{(2)}$ obtained from N_1 , N_5 , and N_{40} using Eq. 1. The dashed lines represent expected dynamics according to Eq. 3 where the initial contrast at $\Delta t \rightarrow 0$ is $\beta_0 = 0.2$. A considerably larger error in N_1 is due to the lower photon count rates. Nevertheless, resolving a single X-ray pulse in XPCS offers a 192 ns temporal resolution in this pulse pattern [19].

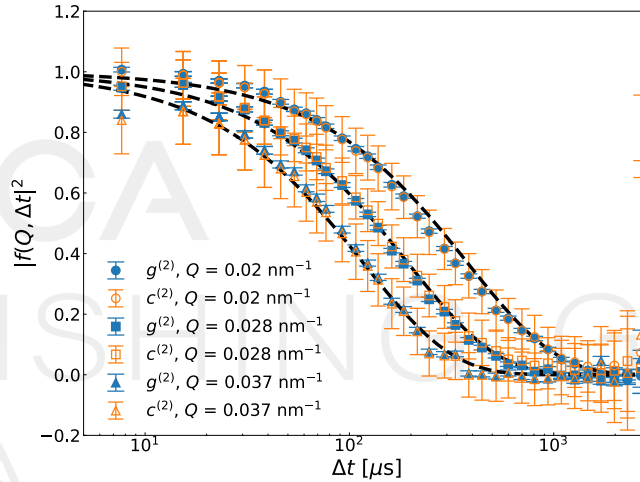


Fig. 4. The obtained intermediate scattering functions from XPCS (circle) and DP-XPCS (square) for varying Q . The black dashed lines represent the expected curves of a single exponential decay curve from Eq. 2.

Figure 4 shows a square of ISF obtained from XPCS ($g^{(2)}$: filled markers) and DP-XPCS ($c^{(2)}$: empty markers) in N_{40} for various Q values. The ISF from $g^{(2)}$ extracted from Eq. 1 decays as a function of delay time representing the motion of silica particles. The obtained initial contrast β_0 from $g^{(2)}$ was employed to Eq. 6 to extract ISF and α from $c^{(2)}$. The black dashed lines represent dynamics of Brownian motion in freely diffusing silica particles in water with the relaxation rate Γ of 1315, 2578, and 4262 s^{-1} at $Q = 0.02, 0.028$, and 0.037 nm^{-1} , respectively.

We calculated speckle contrast as a function of exposure time to obtain the X-ray speckle visibility using the normalized variance. In contrast to the XPCS and DP-XPCS, the image $I^V(Q, t_e)$ for XSVS is a result of the summation of all the memory cells between the corresponding delay time. Figure 5 shows speckle visibility contrast as red squares for $Q = 0.02$ (a), 0.028 (b), and 0.037 (c), respectively. Also, XPCS results are shown as blue circles at corresponding Q in N_{40} . The dotted and dashed lines for the XPCS and XSVS experiment are the fit using Eq. 3 and Eq. 5, respectively. The extracted Γ as a function of wavevector transfer is in excellent agreement for all three approaches. This result shows that all the methods are well suited for pulsed-based studies.

Dynamics measured via pulsed-based XPCS in a model colloidal model system of silica

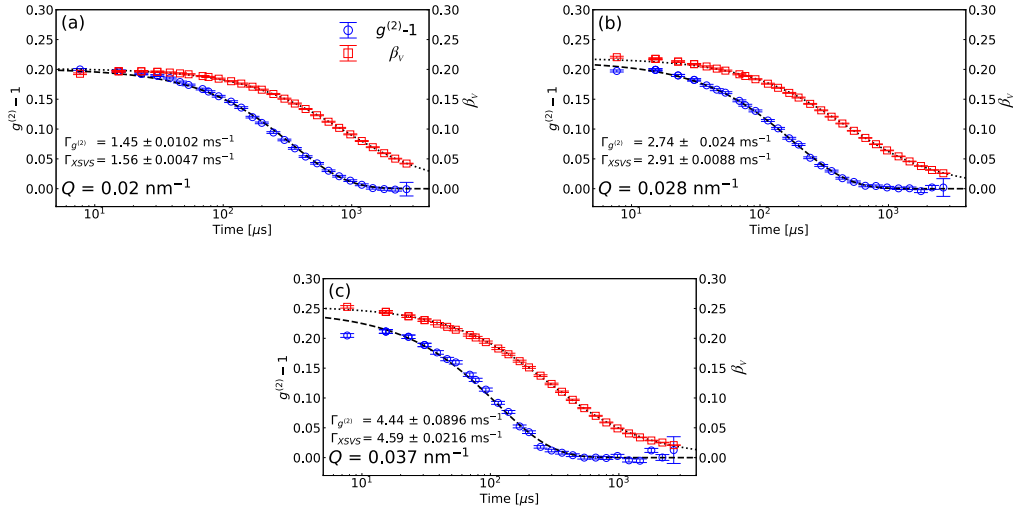


Fig. 5. Combined XPCS $g^{(2)}-1$ and speckle visibility contrast β_v at the wavevector transfer Q of (a) 0.02 nm^{-1} , (b) 0.028 nm^{-1} , (c) 0.037 nm^{-1} . The dashed and dotted lines are the fit result using Eq. 3 and Eq. 5, respectively.

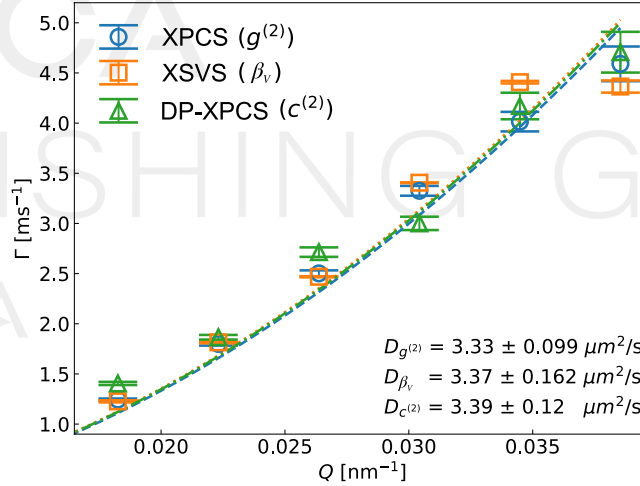


Fig. 6. Extracted Γ as a function of Q . The lines are the fitting results using $\Gamma(Q) = D_0 Q^2$.

157 particles in water mark an important step in adopting various pulse patterns of storage rings in
 158 XPCS measurements. A higher coherent flux available with diffraction-limited storage rings
 159 (DLSR) will extend the access to study weakly scattering, but very relevant systems [54]. The
 160 possibility of employing a time structure of DLSRs paves the way to studying dynamics on
 161 nanosecond to microsecond timescales bridging the experimental gap between 3rd generation
 162 synchrotron sources and XFEL sources in investigating more complex systems, in particular, fast
 163 relaxation processes in glasses [11], atomic diffusion in metal alloys [55], soft matter [20] and
 164 biological systems [56].

4. Conclusions

We have demonstrated pulsed XPCS at a synchrotron source by employing various pulse patterns of PETRA III. The diffusion coefficients obtained from the three speckle correlation techniques, i.e., XPCS, XSVS, and DP-XPCS, show very good agreement with the expected dynamics of the colloidal system. The SPARTA detector capability of MHz frame rates has provided a way of conducting such experiments with very short time resolutions, spanning the range from 190 ns over microseconds to milliseconds to cover a fast but also wide range of times in correlation functions. These studies will provide great potential for X-ray speckle-based investigation for all synchrotron facilities operated by individual X-ray repetition rates and, in particular, diffraction-limited storage rings.

Disclosures. The authors declare no conflicts of interest.

Data availability. Data underlying the results presented in this paper are not publicly available at this time but may be obtained from the authors upon reasonable request.

Supplemental document. See Supplement 1 for supporting content.

References

1. B. J. Berne and R. Pecora, *Dynamic Light Scattering* (John Wiley, New York, 1976).
2. D. K. Carpenter, "Dynamic light scattering with applications to chemistry, biology, and physics," *J. Chem. Educ.* **54**, A430 (1977).
3. P. Zakharov, S. Bhat, P. Schurtenberger, and F. Scheffold, "Multiple-scattering suppression in dynamic light scattering based on a digital camera detection scheme," *Appl. Opt.* **45**, 1756 (2006).
4. S. O. Hruszkewycz, M. Sutton, P. H. Fuoss, B. Adams, S. Rosenkranz, K. F. Ludwig, W. Roseker, D. Fritz, M. Cammarata, D. Zhu, S. Lee, H. Lemke, C. Gutt, A. Robert, G. Grübel, and G. B. Stephenson, "High contrast x-ray speckle from atomic-scale order in liquids and glasses," *Phys. Rev. Lett.* **109**, 185502 (2012).
5. E. F. Semeraro, J. Möller, and T. Narayanan, "Multiple-scattering effects in SAXS and XPCS measurements in the ultra-small-angle region," *J. Appl. Crystallogr.* **51**, 706–713 (2018).
6. S. B. Dierker, R. Pindak, R. M. Fleming, I. K. Robinson, and L. Berman, "X-Ray Photon Correlation Spectroscopy Study of Brownian Motion of Gold Colloids in Glycerol," *Phys. Rev. Lett.* **75**, 449–452 (1995).
7. G. Grübel and F. Zontone, "Correlation spectroscopy with coherent x-rays," *J. Alloy. Compd.* **362**, 3–11 (2004).
8. F. Lehmkuhler, J. Valerio, D. Sheyfer, W. Roseker, M. A. Schroer, B. Fischer, K. Tono, M. Yabashi, T. Ishikawa, and G. Grübel, "Dynamics of soft nanoparticle suspensions at hard X-ray FEL sources below the radiation-damage threshold," *IUCrJ* **5**, 801–807 (2018).
9. L. Frenzel, F. Lehmkuhler, I. Lokteva, S. Narayanan, M. Sprung, and G. Grübel, "Anomalous Dynamics of Concentrated Silica-PNIPAm Nanogels," *The J. Phys. Chem. Lett.* **10**, 5231–5236 (2019).
10. C. Gutt, T. Ghaderi, V. Chamard, A. Madsen, T. Seydel, M. Tolan, M. Sprung, G. Grübel, and S. K. Sinha, "Observation of Heterodyne Mixing in Surface X-Ray Photon Correlation Spectroscopy Experiments," *Phys. Rev. Lett.* **91**, 076104 (2003).
11. B. Ruta, Y. Chushkin, G. Monaco, L. Cipelletti, E. Pineda, P. Bruna, V. M. Giordano, and M. Gonzalez-Silveira, "Atomic-scale relaxation dynamics and aging in a metallic glass probed by X-ray photon correlation spectroscopy," *Phys. Rev. Lett.* **109**, 165701 (2012).
12. Z. Evenson, B. Ruta, S. Hechler, M. Stolpe, E. Pineda, I. Gallino, and R. Busch, "X-Ray Photon Correlation Spectroscopy Reveals Intermittent Aging Dynamics in a Metallic Glass," *Phys. Rev. Lett.* **115**, 175701 (2015).
13. Y. Chushkin, C. Caronna, and A. Madsen, "A novel event correlation scheme for X-ray photon correlation spectroscopy," *J. Appl. Crystallogr.* **45**, 807–813 (2012).
14. F. Perakis, K. Amann-Winkel, F. Lehmkuhler, M. Sprung, D. Mariedahl, J. A. Sellberg, H. Pathak, A. Späh, F. Cavalca, D. Schlesinger, A. Ricci, A. Jain, B. Massani, F. Aubree, C. J. Benmore, T. Loerting, G. Grübel, L. G. M. Pettersson, and A. Nilsson, "Diffusive dynamics during the high-to-low density transition in amorphous ice," *Proc. National Acad. Sci.* **114**, 8193–8198 (2017).
15. A. K. Rumaiz, D. P. Siddons, G. Deptuch, P. Maj, A. J. Kuczewski, G. A. Carini, S. Narayanan, E. M. Dufresne, A. Sandy, R. Bradford, A. Flueraşu, and M. Sutton, "First experimental feasibility study of VIPIC: a custom-made detector for X-ray speckle measurements," *J. Synchrotron Radiat.* **23**, 404–409 (2016).
16. Q. Zhang, E. M. Dufresne, S. Narayanan, P. Maj, A. Koziol, R. Szczygiel, P. Grybos, M. Sutton, and A. R. Sandy, "Sub-microsecond-resolved multi-speckle X-ray photon correlation spectroscopy with a pixel array detector," *J. Synchrotron Radiat.* **25**, 1408–1416 (2018).
17. S. Berkowicz, S. Das, M. Reiser, M. Filianina, M. Bin, G. Crevatin, F. Hennies, C. Weninger, A. Björling, P. Bell, and F. Perakis, "Nanofocused x-ray photon correlation spectroscopy," *Phys. Rev. Res.* **4**, L032012 (2022).

- 220 18. K. Switalski, J. Fan, L. Li, M. Chu, E. Sarnello, P. Jemian, T. Li, Q. Wang, and Q. Zhang, "Direct measurement of
221 stokes-einstein diffusion of cowpea mosaic virus with 19 μ s-resolved xpcs," *J. synchrotron radiation* **29**, 1429–1435
222 (2022).
- 223 19. W. Jo, F. Westermeier, R. Rysov, O. Leupold, F. Schulz, S. Tober, V. Markmann, M. Sprung, A. Ricci, T. Laurus,
224 A. Aschkan, A. Klyuev, U. Trunk, H. Graafsma, G. Grübel, and W. Roseker, "Nanosecond X-ray photon correlation
225 spectroscopy using pulse time structure of a storage-ring source," *IUCr* **8**, 124–130 (2021).
- 226 20. F. Lehmkuhler, F. Dallari, A. Jain, M. Sikorski, J. Möller, L. Frenzel, I. Lokteva, G. Mills, M. Walther, H. Sinn,
227 F. Schulz, M. Dartsch, V. Markmann, R. Bean, Y. Kim, P. Vagovic, A. Madsen, A. P. Mancuso, and G. Grübel,
228 "Emergence of anomalous dynamics in soft matter probed at the european xfel," *Proc. National Acad. Sci.* **117**,
229 24110–24116 (2020).
- 230 21. F. Dallari, M. Reiser, I. Lokteva, A. Jain, J. Möller, M. Scholz, A. Madsen, G. Grübel, F. Perakis, and F. Lehmkuhler,
231 "Analysis strategies for mhz xpcs at the european xfel," *Appl. Sci.* **11** (2021).
- 232 22. R. Bandyopadhyay, A. S. Gittings, S. S. Suh, P. K. Dixon, and D. J. Durian, "Speckle-visibility spectroscopy: A tool
233 to study time-varying dynamics," *Rev. Sci. Instruments* **76**, 093110 (2005).
- 234 23. I. Inoue, Y. Shinohara, A. Watanabe, and Y. Amemiya, "Effect of shot noise on x-ray speckle visibility spectroscopy,"
235 *Opt. Express* **20**, 26878–26887 (2012).
- 236 24. L. Li, P. Kwaśniewski, D. Orsi, L. Wiegart, L. Cristofolini, C. Caronna, and A. Flueraşu, "Photon statistics and
237 speckle visibility spectroscopy with partially coherent X-rays," *J. Synchrotron Radiat.* **21**, 1288–1295 (2014).
- 238 25. F. Perakis, G. Camisasca, T. J. Lane, A. Späh, K. T. Wikfeldt, J. A. Sellberg, F. Lehmkuhler, H. Pathak, K. H. Kim,
239 K. Amann-Winkel, S. Schreck, S. Song, T. Sato, M. Sikorski, A. Eilert, T. McQueen, H. Ogasawara, D. Nordlund,
240 W. Roseker, J. Koralek, S. Nelson, P. Hart, R. Alonso-Mori, Y. Feng, D. Zhu, A. Robert, G. Grübel, L. G. M.
241 Pettersson, and A. Nilsson, "Coherent X-rays reveal the influence of cage effects on ultrafast water dynamics," *Nat.*
242 *Commun.* **9**, 1917 (2018).
- 243 26. J. Möller, M. Reiser, J. Hallmann, U. Boesenberg, A. Zozulya, H. Rahmann, A.-L. Becker, F. Westermeier, T. Zinn,
244 F. Zontone, C. Gutt, and A. Madsen, "Implications of disturbed photon-counting statistics of Eiger detectors for
245 X-ray speckle visibility experiments," *J. Synchrotron Radiat.* **26**, 1705–1715 (2019).
- 246 27. J. Möller, M. Reiser, J. Hallmann, U. Boesenberg, A. Zozulya, H. Rahmann, A.-L. Becker, F. Westermeier, T. Zinn,
247 M. Sprung, T. Narayanan, C. Gutt, and A. Madsen, "Using low dose x-ray speckle visibility spectroscopy to study
248 dynamics of soft matter samples," *New J. Phys.* **23**, 093041 (2021).
- 249 28. C. Gutt, L.-M. Stadler, A. Duri, T. Autenrieth, O. Leupold, Y. Chushkin, and G. Grübel, "Measuring temporal speckle
250 correlations at ultrafast x-ray sources," *Opt. Express* **17**, 55–61 (2009).
- 251 29. S. Lee, W. Jo, H. S. Wi, C. Gutt, and G. W. Lee, "Resolving high-speed colloidal dynamics beyond detector response
252 time via two pulse speckle contrast correlation," *Opt. Express* **22**, 21567–21576 (2014).
- 253 30. M. H. Seaberg, B. Holladay, J. C. T. Lee, M. Sikorski, A. H. Reid, S. A. Montoya, G. L. Dakovski, J. D. Koralek,
254 G. Coslovich, S. Moeller, W. F. Schlotter, R. Streubel, S. D. Kevan, P. Fischer, E. E. Fullerton, J. L. Turner, F.-J.
255 Decker, S. K. Sinha, S. Roy, and J. J. Turner, "Nanosecond x-ray photon correlation spectroscopy on magnetic
256 skyrmions," *Phys. Rev. Lett.* **119**, 067403 (2017).
- 257 31. Y. Sun, F.-J. Decker, J. Turner, S. Song, A. Robert, and D. Zhu, "Pulse intensity characterization of the LCLS
258 nanosecond double-bunch mode of operation," *J. Synchrotron Radiat.* **25**, 642–649 (2018).
- 259 32. W. Roseker, H. Franz, H. Schulte-Schrepping, A. Ehnes, O. Leupold, F. Zontone, A. Robert, and G. Grübel,
260 "Performance of a picosecond x-ray delay line unit at 8.39 keV," *Opt. Lett.* **34**, 1768–1770 (2009).
- 261 33. W. Roseker, H. Franz, H. Schulte-Schrepping, A. Ehnes, O. Leupold, F. Zontone, S. Lee, A. Robert, and G. Grübel,
262 "Development of a hard X-ray delay line for X-ray photon correlation spectroscopy and jitter-free pump-probe
263 experiments at X-ray free-electron laser sources," *J. Synchrotron Radiat.* **18**, 481–491 (2011).
- 264 34. W. Roseker, S. O. Hruszkewycz, F. Lehmkuhler, M. Walther, H. Schulte-Schrepping, S. Lee, T. Osaka, L. Strüder,
265 R. Hartmann, M. Sikorski, S. Song, A. Robert, P. H. Fuoss, M. Sutton, G. B. Stephenson, and G. Grübel, "Towards
266 ultrafast dynamics with split-pulse x-ray photon correlation spectroscopy at free electron laser sources," *Nat. Commun.*
267 **9**, 1704 (2018).
- 268 35. Y. Sun, M. Dunne, P. Fuoss, A. Robert, D. Zhu, T. Osaka, M. Yabashi, and M. Sutton, "Realizing split-pulse x-ray
269 photon correlation spectroscopy to measure ultrafast dynamics in complex matter," *Phys. Rev. Res.* **2**, 023099 (2020).
- 270 36. J. Sakamoto, K. Ohwada, M. Ishino, J. Mizuki, M. Ando, and K. Namikawa, "Design of a prototype split-and-delay
271 unit for XFEL pulses, and their evaluation by synchrotron radiation X-rays," *J. Synchrotron Radiat.* **24**, 95–102
272 (2017).
- 273 37. W. Lu, T. Noll, T. Roth, I. Agapov, G. Geloni, M. Holler, J. Hallmann, G. Ansaldo, S. Eisebitt, and A. Madsen,
274 "Design and throughput simulations of a hard x-ray split and delay line for the mid station at the european xfel," *AIP*
275 *Conf. Proc.* **1741**, 030010 (2016).
- 276 38. W. Lu, B. Friedrich, T. Noll, K. Zhou, J. Hallmann, G. Ansaldo, T. Roth, S. Serkez, G. Geloni, A. Madsen, and
277 S. Eisebitt, "Development of a hard x-ray split-and-delay line and performance simulations for two-color pump-probe
278 experiments at the european xfel," *Rev. Sci. Instruments* **89**, 063121 (2018).
- 279 39. T. Hirano, T. Osaka, Y. Morioka, Y. Sano, Y. Inubushi, T. Togashi, I. Inoue, S. Matsuyama, K. Tono, A. Robert,
280 J. B. Hastings, K. Yamauchi, and M. Yabashi, "Performance of a hard X-ray split-and-delay optical system with a
281 wavefront division," *J. Synchrotron Radiat.* **25**, 20–25 (2018).
- 282 40. T. Osaka, T. Hirano, Y. Sano, Y. Inubushi, S. Matsuyama, K. Tono, T. Ishikawa, K. Yamauchi, and M. Yabashi,

- 283 “Wavelength-tunable split-and-delay optical system for hard x-ray free-electron lasers,” *Opt. Express* **24**, 9187–9201
284 (2016).
- 285 41. T. Osaka, T. Hirano, Y. Morioka, Y. Sano, Y. Inubushi, T. Togashi, I. Inoue, K. Tono, A. Robert, K. Yamauchi, J. B.
286 Hastings, and M. Yabashi, “Characterization of temporal coherence of hard X-ray free-electron laser pulses with
287 single-shot interferograms,” *IUCrJ* **4**, 728–733 (2017).
- 288 42. H. Li, Y. Sun, J. Vila-Comamala, T. Sato, S. Song, P. Sun, M. H. Seaberg, N. Wang, J. B. Hastings, M. Dunne,
289 P. Fuoss, C. David, M. Sutton, and D. Zhu, “Generation of highly mutually coherent hard-x-ray pulse pairs with an
290 amplitude-splitting delay line,” *Phys. Rev. Res.* **3**, 043050 (2021).
- 291 43. A. V. Zozulya, A. Shabalin, H. Schulte-Schrepping, J. Heuer, M. Spiwek, I. Sergeev, I. Besedin, I. A. Vartanyants, and
292 M. Sprung, “Wavefront preserving channel-cut optics for coherent x-ray scattering experiments at the P10 beamline
293 at PETRAIII,” *J. Physics: Conf. Ser.* **499**, 012003 (2014).
- 294 44. X. Shi, R. Dinapoli, B. Henrich, A. Mozzanica, B. Schmitt, R. Mazzocco, H. Krüger, U. Trunk, and H. Graafsma,
295 “Challenges in chip design for the AGIPD detector,” *Nucl. Instruments Methods Phys. Res. Sect. A: Accel.*
296 *Spectrometers, Detect. Assoc. Equip.* **624**, 387–391 (2010).
- 297 45. D. Mezza, A. Allahgholi, G. Arino-Estrada, L. Bianco, A. Delfs, R. Dinapoli, P. Goettlicher, H. Graafsma,
298 D. Greiffenberg, H. Hirsemann, S. Jack, R. Klanner, A. Klyuev, H. Krueger, A. Marras, A. Mozzanica, J. Poehlsen,
299 B. Schmitt, J. Schwandt, I. Sheviakov, X. Shi, U. Trunk, Q. Xia, J. Zhang, and M. Zimmer, “Characterization of
300 AGIPD1.0: The full scale chip,” *Nucl. Instruments Methods Phys. Res. Sect. A: Accel. Spectrometers, Detect. Assoc.*
301 *Equip.* **838**, 39–46 (2016).
- 302 46. D. Mezza, A. Allahgholi, A. Delfs, R. Dinapoli, P. Goettlicher, H. Graafsma, D. Greiffenberg, H. Hirsemann,
303 A. Klyuev, T. Laurus, A. Marras, A. Mozzanica, I. Perova, J. Poehlsen, B. Schmitt, I. Sheviakov, X. Shi, U. Trunk,
304 Q. Xia, J. Zhang, and M. Zimmer, “New calibration circuitry and concept for AGIPD,” *J. Instrum.* **11**, C11019–C11019
305 (2016).
- 306 47. A. J. F. Siegert, “On the fluctuations in signals returned by many independently moving scatters,” Report No. **465**
307 (Radiation laboratory, Massachusetts Institute of Technology, 1943).
- 308 48. D. Ferreira, R. Bachelard, W. Guerin, R. Kaiser, and M. Fouché, “Connecting field and intensity correlations: The
309 siegert relation and how to test it,” *Am. J. Phys.* **88**, 831–837 (2020).
- 310 49. J. Möller, M. Sprung, A. Madsen, and C. Gutt, “X-ray photon correlation spectroscopy of protein dynamics at nearly
311 diffraction-limited storage rings,” *IUCrJ* **6**, 794–803 (2019).
- 312 50. F. Lehmkuhler, W. Roseker, and G. Grübel, “From femtoseconds to hours—measuring dynamics over 18 orders of
313 magnitude with coherent x-rays,” *Appl. Sci.* **11** (2021).
- 314 51. P. K. Dixon and D. J. Durian, “Speckle visibility spectroscopy and variable granular fluidization,” *Phys. Rev. Lett.* **90**,
315 184302 (2003).
- 316 52. C. DeCaro, V. N. Karunaratne, S. Bera, L. B. Lurio, A. R. Sandy, S. Narayanan, M. Sutton, J. Winans, K. Duffin,
317 J. Lehuta, and N. Karonis, “X-ray speckle visibility spectroscopy in the single-photon limit,” *J. Synchrotron Radiat.*
318 **20**, 332–338 (2013).
- 319 53. J. Goodman, *Speckle Phenomena in Optics: Theory and Applications* (Roberts & Company, 2007).
- 320 54. K. H. Kim, A. Späh, H. Pathak, F. Perakis, D. Mariedahl, K. Amann-Winkel, J. A. Sellberg, J. H. Lee, S. Kim, J. Park,
321 K. H. Nam, T. Katayama, and A. Nilsson, “Maxima in the thermodynamic response and correlation functions of
322 deeply supercooled water,” *Science* **358**, 1589–1593 (2017).
- 323 55. M. Leitner, B. Sepiol, L.-M. Stadler, B. Pfau, and G. Vogl, “Atomic diffusion studied with coherent x-rays,” *Nat.*
324 *Mater.* **8**, 717–720 (2009).
- 325 56. A. Girelli, H. Rahmann, N. Begam, A. Ragulskaya, M. Reiser, S. Chandran, F. Westermeier, M. Sprung, F. Zhang,
326 C. Gutt, and F. Schreiber, “Microscopic dynamics of liquid-liquid phase separation and domain coarsening in a
327 protein solution revealed by x-ray photon correlation spectroscopy,” *Phys. Rev. Lett.* **126**, 138004 (2021).